

## Engineering the bundled glass column: From the design concept to full-scale experimental testing

Oikonomopoulou, Faidra; van den Broek, E.A.M.; Bristogianni, Telesilla; Veer, Fred; Nijssse, Rob

**Publication date**

2017

**Document Version**

Proof

**Published in**

Intelligent Glass Solutions

**Citation (APA)**

Oikonomopoulou, F., van den Broek, E. A. M., Bristogianni, T., Veer, F., & Nijssse, R. (2017). Engineering the bundled glass column: From the design concept to full-scale experimental testing. *Intelligent Glass Solutions*, 58-65.

**Important note**

To cite this publication, please use the final published version (if applicable).  
Please check the document version above.

**Copyright**

Other than for strictly personal use, it is not permitted to download, forward or distribute the text or part of it, without the consent of the author(s) and/or copyright holder(s), unless the work is under an open content license such as Creative Commons.

**Takedown policy**

Please contact us and provide details if you believe this document breaches copyrights.  
We will remove access to the work immediately and investigate your claim.

# Engineering the bundled glass column: From the design concept to full-scale experimental testing



ir. Faidra Oikonomopoulou, TUDelft

## Abstract

This article gives an overview of the research conducted by the authors from the design concept to the engineering and full-scale testing of the bundled glass column. Consisting of adhesively bonded solid glass rods, the bundled column is a promising solution for transparent compressive members. To

investigate the feasibility of the bundled column for real applications, a production method is developed first for manufacturing specimens with guaranteed, consistent structural and visual performance. The final column consists of six solid circular rods adhesively bonded to a central star-shaped profile by a clear, UV-curing adhesive. To

validate the design, series of prototypes up to 2.4 m long are made and tested in compression. With the aim of securing a more gradual and thus safer failure, a post-tensioned steel tendon is introduced to one of the 2.4 m long series and experimentally evaluated. The results demonstrate that the chosen adhesive and rod configuration enable the designed column to

perform monolithically under loading and fail in values close to the theoretical buckling force. The results of the post-tensioned specimens suggest that post-tensioning allows for a more ductile and more consistent failure, which in turn can allow reduced safety factors. Based on the findings, suggestions are made for the further engineering of the bundled column.

## Introduction

Transparency in combination with durability and a compressive strength higher than that of wood, concrete and even steel, have rendered glass the ideal candidate for realizing transparent structural components. Despite the material's inherent brittleness, advancements in glass technologies and engineering over the last decades have rendered glass structures safe and reliable. From the works of Peter Rice in Cite des Sciences et de l'Industrie at Parc de la Vilette 30 years ago to the all-glass structures by Eckersley O'Callaghan engineers, glass has gained the trust of many engineers as a structural material: the glass elements become larger and the connections become less, both in size and number. The long pursued architectural desire for a pure glass structure is finally feasible.

Although the application of glass is constantly increasing in load-bearing beams, portals and buildings skins, free-standing all-glass columns are still in an early stage of development. Realized examples of free-standing glass columns can be counted on the fingers of one hand. The cruciform columns that support a glass patio at St-Fermain-en-Laye in France (Schittich et al. 2007) and the reception building at Danfoss Headquarters in Denmark (Bagger, Petersen 2009) are the two most characteristic projects. In both examples, the inclusion of the cruciform glass columns in the building was only possible after performing 1:1 scale testing to demonstrate that they are able to carry at least double the required compressive forces. Also, in both cases, the engineers had to design the roof with sufficient redundancy to redistribute the forces in case of a column's complete failure (Bagger, Petersen 2009; Nijse 2003). These two examples demonstrate both the challenges and the potential of all-glass columns: increased safety factors and alternative load paths are prerequisites for the realization of glass columns to compensate for their lack of a built-in safety system. Nonetheless, the architectural potential of such compressive members is vast:

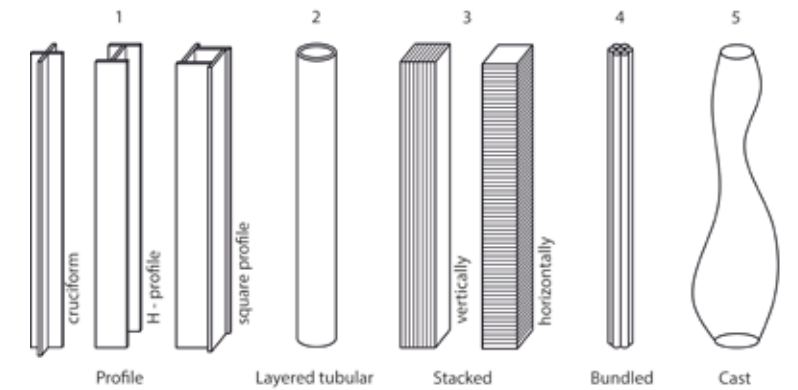


Fig.1: Illustration of the five different types of all glass columns as described by (Nijse,ten Brincke 2014).

Forming almost invisible vertical members, glass columns provide a promising solution for continuous, uninterrupted spaces, sparing the necessity of expensive, column-free structural solutions.

Over the last years, these possibilities coupled with the engineering puzzles of fabricating a safe all glass column have triggered various researchers. Different conceptual designs have been explored, summarized by (Nijse,ten Brincke 2014) in five categories: profile, layered tubular, stacked, cast, and bundled (see fig.1).

Bundled columns are one of the least explored ideas. This promising concept was first introduced by (Nijse 2003) as a safe, all glass column made of a bundle of solid glass bars that are adhesively bonded together. In terms of visual performance, the bundled glass column is transparent, yet not invisible. The curved geometry of the rods results in playful distortions and light reflections, subtly revealing the column's existence (Oikonomopoulou et al. 2016). The idea was initially conceived for the office of the ABT engineers in Arnhem: 7 solid glass rods, 30 mm in diameter, are bonded together by a transparent adhesive so that the central one is surrounded by the other six. However, the column was never realized due to difficulties in establishing a bonding method that would ensure consistency both in terms of visual and structural performance.

## Engineering steps towards the realization of the bundled column

This article gives an overview of the research conducted by the authors from the design concept to the engineering and full-scale testing of the bundled glass column. The concept of the bundled column is in itself

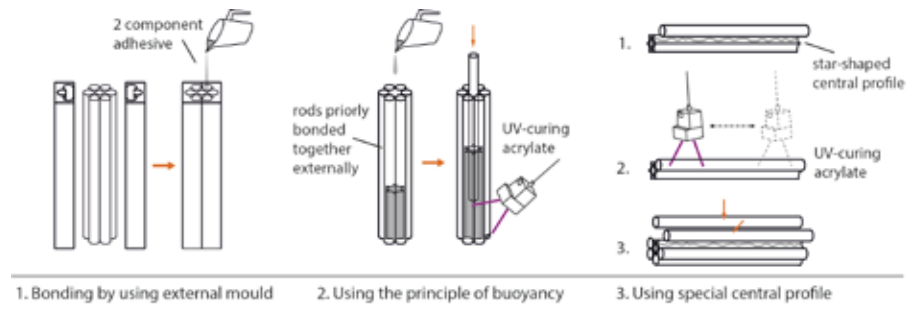


Fig.2: Realized 1.5m long prototypes of the bundled column by the authors

simple: Multiple glass bars are bonded together by a colourless adhesive, forming a composite yet unified cross-section. The column's load-bearing capacity is enhanced by the symmetrical cross-section of both the individual rods and of the final, composite section. In this context, solid rods with a circular cross-section are selected due to their inherent resistance in both buckling and torsion. To investigate the feasibility of the bundled column for real applications, first a production method is developed for manufacturing specimens in a scale relevant to buildings with guaranteed consistency in their structural and visual performance. Following, series of prototypes up to 2.4 m in height are made and tested in compression. With the aim of a more gradual and thus safer failure, a post-tensioned steel tendon is introduced to one of the 2.4 m long series and experimentally evaluated. Based on the findings, suggestions are made for the further engineering of the bundled column.

### Production challenges and solutions in the design phase

Initially, different glass rod configurations, adhesives and bonding techniques were explored in search of a combination that would (a) ensure the desired coupling degree or the individual rods, (b) achieve minimum visual unevenness and (c) result to an easy and standardized manufacturing method. Fig. 3 illustrates the main bonding techniques and configurations explored.



**Fig.3: Illustration of the explored bonding techniques and rod configurations.**

Extruded borosilicate profiles by SCHOTT are used, as they are available in standardized 1500 mm long units up to 30 ( $\pm 0.80$ ) mm in diameter (SCHOTT 2012). The first two bonding methods (see fig.3), proposing a bundled column made out of seven identical rods, were both discarded as they could not account for any intolerances in the standard diameter of the rods. This would result in the custom fabrication of each column unit and/or to columns with decreased strength and visible optical distortions in the adhesive bond (Oikonomopoulou et al. 2016). The necessity of a standardized, universal production method that can guarantee consistent quality lead to the third bonding technique and rod configuration.

The third and final method proposes a new rod configuration: a central, star-shaped, hollow CONTURAX® profile is surrounded by 6 DURAN® rods. The latter have a diameter corresponding to the convex of the flutes of the central star profile. Since the CONTURAX® profile is only commercially available with a 17 ( $\pm 2.00$ ) mm inner and 30 ( $\pm 2.00$ ) mm external diameter (SCHOTT AG 2013), the 6 external DURAN® rods have a diameter of 22 ( $\pm 0.45$ ) mm in order to match the flute's convex surfaces. Despite the size tolerances of the individual components, the construction of several prototypes verified that the matching curvature between the rods and the flutes of the central profile is sufficient for guaranteeing strong bonds with minimum, if any, visual distortions (Oikonomopoulou et al. 2016). The final configuration can be seen in fig.4.

### Adhesive selection and degree of coupling of the rods

The adhesive connection between adjacent glass components is fundamental for the overall structural performance of the glass column. The higher the bonding strength, the more the elements couple, preventing individual buckling. Delo Photobond 4468,



**Fig.4: Rod configuration of the final bundled column design.**



**Fig.5: The 500 mm long specimen series tested in compression.**



**Fig.6: Left: Experimental set-up for the testing of alternative connections. Right: Specimens comprising two continuous rods and one interrupted in the middle.**

a one-component, clear, UV-curing acrylate, was chosen due to its colourless nature, similar refraction index to glass, fast application and very good mechanical properties (Delo Industrial Adhesives 2014). This low viscosity adhesive can only be applied in a horizontal strip along the length of each flute of the central profile. Accordingly, the circular rods are bonded one by one in a horizontal position, by fully curing the adhesive using 60mW/cm<sup>2</sup> UVA intensity in a minimum of 40 seconds (Delo Industrie Klebstoffe 2014). The homogeneous distribution and spread of the adhesive, as well as its similar refraction index to glass result in minimal visual distortion.

Previous 4-point bending experiments by (Oikonomopoulou et al. 2015) on glass beams consisting of adhesively bonded solid glass bricks by the same adhesive demonstrated a monolithic behaviour of the assembly under loading. In the case of the bundled column, the degree of coupling was evaluated by performing compression tests in a series of three 500 mm long specimens of the proposed bundle (see fig.5). All specimens failed at a consistent stress of approximately 500 MPa, indicating that the high shear stiffness of the selected adhesive enables the bundle to behave monolithically under compressive forces less than 1000 kN.

**Scaling up: Spliced lamination principle**  
SCHOTT's extruded profiles are standardized

up to 1500 mm length. Communication with the manufacturer indicated that longer profiles (up to 10000 mm) are possible but require a specialized order for above 500 units. Since the first phase of research dealt with a limited amount of profiles, an alternative, and more economic, method was sought for producing specimens longer than 1500 mm. In specific, longer components were made by adapting the spliced lamination principle: To prevent the generation of weaker zones, each column is segmented in such a way that the connection points spiral up along its height. To optimize material use, every split point of the spiral splice-lamination has a 250 mm absolute height distance from the next split point of the adjacent rod. Three different connection types, a small gap, an adhesive connection by Delo Photobond 4494 and a 2mm thick aluminium

disc, were experimentally tested in a series of 470 mm long specimens. Each specimen comprised three rods, two continuous and one interrupted in the middle, in order to evaluate the degree of influence of the split lamination joint. The results were compared with those of monolithic specimens of the same configuration. The mock ups and experimental set-up can be seen in fig.6.

The results indicated that the specimens with an aluminium ring in their split joint, bonded with Delo Photobond 4468 to the glass surfaces, perform at the closest approximation to the bundle with continuous rods – on average at 86% of the latter's structural performance. Thus, aluminium discs were used for the split joints of the 2.4 m long spliced specimens.



**Fig.7: Detail of the aluminium disc used for the spliced-lamination scheme.**

**Experimental testing of full-scale specimens**

Based on the findings described above, two series of 2.4 m long specimens are made and tested in compression until failure, namely the NT and the PT series, in order to investigate the load-bearing capacity and failure behaviour of the standard, non-tensioned (NT), and the post-tensioned (PT) column. Thus, in the NT series, the prototypes are made solely out of the glass bundle (NT specimens) whilst in the PT series, the specimens include an axial post-tensioned steel tendon with the aim of attaining a more gradual, visible and predictable buckling failure (PT specimens).

Each series comprises three identical specimens, consisting of 6 borosilicate DURAX® rods of  $\varnothing 22(\pm 0.45)$  mm adhesively bonded by Delo Photobond 4468 to a central hollow star-shaped CONTURAX® borosilicate glass profile with  $17(\pm 2.00)$  mm inner and  $30(\pm 2.00)$  mm external diameter, as shown in fig.4. To achieve a length of 2.4 m, the specimens follow the previously-described spliced lamination scheme with aluminium discs in the joints. Accordingly, the rods are cut to the desired lengths by a diamond blade saw and are then ground to minimize imperfections at the joining surface with the aluminium disc. Once all rods have been carefully bonded to the star-shaped central profile by the UV-curing adhesive, the top and bottom surfaces are manually ground again to remove any protrusions and form a flat surface. The material and geometry properties of the bundle are summarized in Table 1.

For the NT series of specimens, two milled aluminium heads are mounted at both ends of each bundle to stabilize it and provide a proper contact surface for the testing machine. Prior to mounting, a 1 mm thick lead layer is placed inside each metal head to allow for the even distribution of the applied compression load (see fig.9). Once the glass bundle is aligned to the centre of the metal head, a two-component clear polyurethane is poured in between, to create a rigid connection between the two elements. After the resin is fully cured, the column is flipped and the other connection is treated the same way.

In the PT specimens, the end connections are realized in a different way to allow for the post-tensioned tendon. The latter is introduced in the hollow core of the central

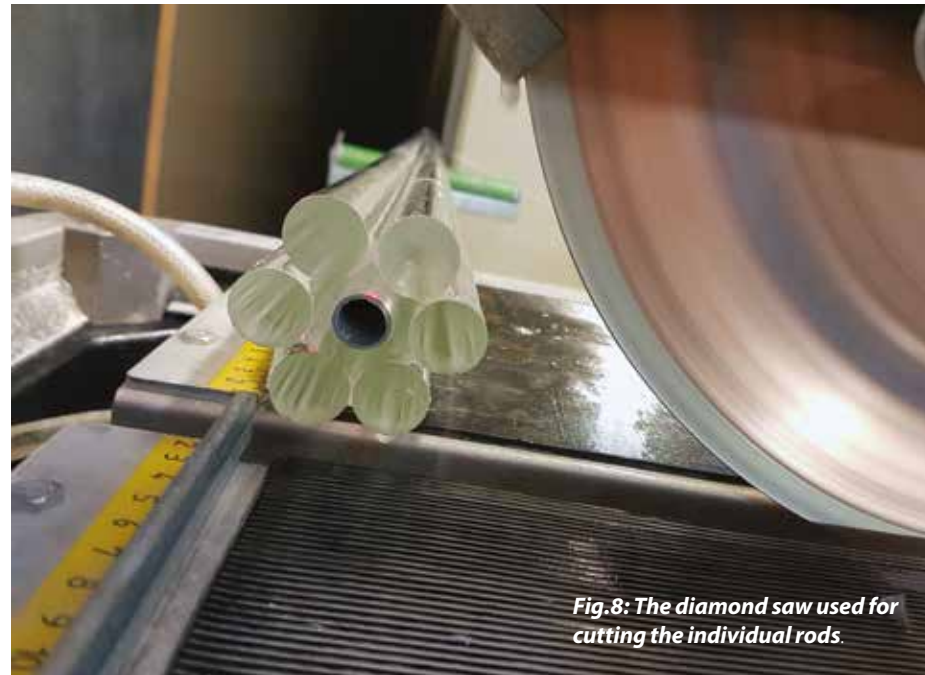


**Fig.8: The diamond saw used for cutting the individual rods.**

Table 1: Material and geometry properties of the glass bundle.		
Property	Symbol	Value
Glass modulus of elasticity	E	64000 N/mm <sup>2</sup>
Glass bundle composition	-	6 x $\varnothing 22$ rods + 1 x star-shape
Length	l	2400 mm
Moment of inertia around minor axis	I	643170 mm <sup>4</sup>
Cross-sectional area of the bundle	A	2552 mm <sup>2</sup>



**Fig.9: Section of a NT specimen showing the top and bottom connection: the glass bundle is incorporated in the aluminium head with a lead interlayer in between.**

star-shaped profile. To account for the  $\pm 2.00$  mm production tolerance in the inner diameter of the star-shaped profile, a standardized M12 threaded rod is used as tendon. A PVC tube of 16mm outer and 13.6 mm inner diameter surrounds the threaded rod to prevent the direct contact between the steel and the glass. Due to the inevitable production deviations of

the CONTURAX® profile, the PVC-coated tendon is not in direct contact with the glass bundle, but as close to it as possible using materials in stock. Based on the steel type, the tendon is post-tensioned to roughly 35 kN of axial force. To accommodate the tendon, the bottom steel cap has an axial hole with a female M12 thread in which the post-tensioned tendon can be

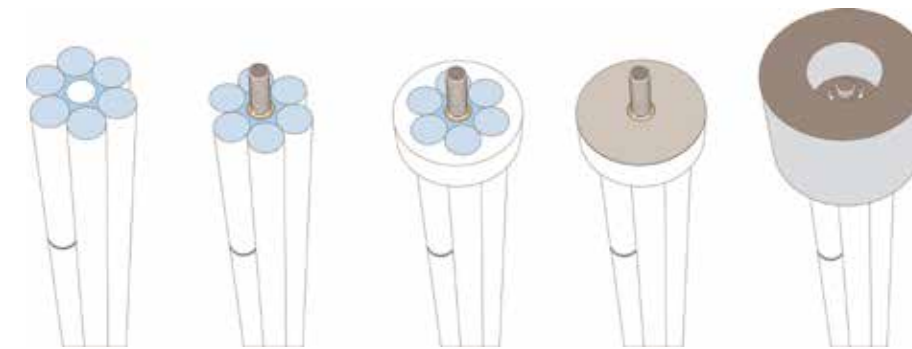


**Fig.10: Illustration of the post-tensioned glass column head detail.**



**Fig.11: Left: Experimental set-up of one of the specimens. Right: Top and bottom pinned connections of the experimental set-up.**

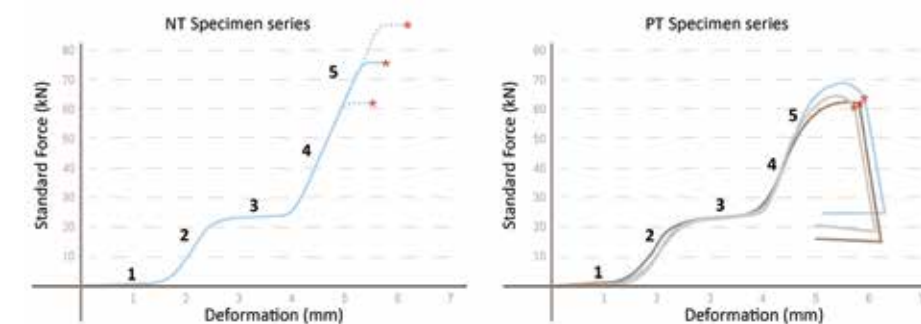


**Fig.12: Left: Indicative load-displacement diagram of the NT specimens. Only the data of one specimen (indicated by the continuous line) were accurately recorded by the compressing machine. The failure of the other two specimens (indicated by dotted lines) is represented here based on the observations and failure load recorded during testing. Right: Load-displacement diagram of the PT specimens (with post-tensioning). In both diagrams: 1:Setting of the machine 2: Column is slightly compressed. 3: Area where the lead layer is compressed. 4: Column is loaded in compression. 5: Initiation of buckling.**

fixed. The top steel cap has a 13 mm hole to allow for the free passage of the tendon, which is tightened with a M12 washer and nut. Again, in these steel heads a 1 mm thick layer of lead is used as intermediary.

All specimens are tested in a pinned configuration. For this, an addition is made to the top and bottom detail: two steel caps with a milled convex and a corresponding half-sphere steel component are placed between the steel surface of the testing machine and the metal ends of the bundled column. The complete specimen is then stabilized by restraining the height of the column through carefully adjusting the machine's top pressing plate until contact is made with negligible introduced force. For safety, all specimens are surrounded by a wooden safety box with a polycarbonate window.

**Results and conclusions**

The load-displacement diagrams of both specimen series and the summary of results can be seen in fig. 12 and Table 2 respectively. The critical load is calculated based on Euler's formula. The influence of the adhesive layer is neglected for the determination of the critical buckling force, as the initial experiments in small prototypes proved that it is safe to assume that the bonded bundle behaves monolithically under loading. The slenderness ratio ( $\lambda$ ) of each specimen series is calculated as the ratio of the effective length of the column to the least radius of gyration ( $r$ ) of its cross section based on Eq. (1).

**Table 2: Dimensions and strength values of the NT (non-post-tensioned) and PT (post-tensioned) series of specimens.**

Series	Spec. No.	Length mm	end connections	Post-tension	Approx. load where first crack was observed	$F_{max}$	$F_{cr}$	$\sigma_{max}$	$\lambda$
						kN	kN	MPa	
NT	1	2400	Pinned	No	45	63.0		24.70	151
	2				N.R.	75.0	70.5	29.40	
	3				70	90.0		35.30	
PT	1	2400	Pinned	Yes	N.R.	69.0		27.00	151
	2				N.R.	64.4	70.5	25.20	
	3				N.R.	62.7		24.60	

**Fig.13: Left: A NT specimen prior and after failure. Right: A PT specimen prior and after failure.**

According to (Kamarudin et al. 2016), glass columns with a slenderness ratio higher than 40 can be classified as slender; hence, they are expected to fail due to buckling. Indeed, all six specimens of both series failed by buckling and out of plane bending at their middle zone, at values in close proximity to the theoretical critical buckling force of 70.5 kN. The spliced joints and eccentricities occurred during fabrication seem to have only a minor influence on the resulting stresses

In specific, the NT specimens failed by buckling in loads ranging between 63 kN and 90

kN. The NT specimens showed sudden and complete failure and had no remaining post-breakage load-carrying capacity (see fig.13). In comparison, the PT specimens failed in a lower yet significantly narrower load range, between 62.7 kN and 69 kN. The specimens of this series demonstrated an increased ductile failure and larger deformations compared to the NT series. Both the consistency in the ultimate stress value, as well as the increased ductile failure mode, can be attributed to the integration of the post-tensioned tendon. In particular, initial crack propagation because of surface defects seems to have been prevented by the

post-tensioning, resulting in more consistent ultimate stress values. Indeed, in contrast to the NT series, where initial cracking was observed in two out of three specimens in a force approx. 20 kN less than the ultimate failure load, here no significant cracking was observed in any specimen prior to failure. Moreover, the PT specimens, in antithesis to the NT ones, had a significantly visible buckling, providing a warning mechanism prior to failure. After failure, the PT specimens maintained a limited load-carrying capacity, attributed mainly to the tendon (see fig.13).

The lower load-bearing capacity of the PT variant is ascribed to the insufficient cooperation between the tendon and the glass, due to inevitable manufacturing tolerances. According to the ACI-318-5 building code by the (American Concrete Institute 2004), a structural member will not buckle under an applied pre-stress if the post-tensioned (coated) tendon is in direct contact with the member. Accordingly, in an ideal scenario, where the glass bundle and the tendon would have been sufficiently in contact to fully collaborate, the tendon would have restrained the glass from moving away from the neutral axis, postponing in this way the initiation of buckling and resulting in higher failure loads compared to the NT variant. In our case, the tolerance of at least 1 mm between the tendon and the bundle prevented the full-cooperation of the two elements. As a result, although the tendon remained in the neutral axis, the glass was free to deviate from the neutral axis of the column once the critical buckling force was reached. Because of this relevant movement, the pre-stress applied by the tendon seems to have contributed to the critical compressive force, triggering buckling already at a load of circa 45 kN and resulting in a seemingly lower failure load. By optimizing the contact between tendon, sheathing and the glass bundle, the lateral movement of the glass bundle leading to eccentricity can be constrained, resulting in higher failure loads.

Still, the visible buckling prior to failure, the consistency in the ultimate stress values and the ability of the PT specimens to withstand complete failure, result in an increased structural reliability. This behaviour allows for the use of lower safety factors and enables the engineering-sound application of the column in buildings. It also demonstrates the potential of the bundled glass column as an elegant and safe solution for transparent, load-bearing compressive members.

With the aim of applying the bundled glass column in future structures, further work will focus on the development of the top and bottom connections as well as on improving the post-tensioning mechanism towards a safer and stronger all-glass column. The presented glass column design will be first applied in the truss elements of a temporary pedestrian 14 m long bridge at the TU Delft campus.

A detailed description of the complete experimental work and the corresponding results can be found in the article: "Design and experimental testing of the bundled glass

column" by the authors, published at the Glass Performance 2017 issue of the Glass Structures & Engineering Journal (<http://link.springer.com/journal/40940/2/2>)

## References

- American Concrete Institute: Building code requirements for structural concrete and commentary. In: ACI 318-05 & ACI 318R-05. American Concrete Institute, US, (2004)
- Bagger, A., Petersen, R.I.: Structural use of glass: Cruciform columns and glass portals with bolted connections subjected to bending. In: Glass Performance Days, Finland 2009, pp. 381-385
- Delo Industrial Adhesives: Technical Information: Delo-Photobond 4468. In: Delo Industrial Adhesives, Windach, (2014)
- Kamarudin, M.K., Disney, P., Parke, G.A.R.: Structural performance of single and bundled glass columns. ARPN Journal of Engineering and Applied Sciences 11(3) (2016)
- Nijse, R.: Glass in Structures: Elements, Concepts, Designs. Birkhauser, Germany (2003)
- Nijse, R., ten Brincke, E.H.J.: Glass columns. In: Louter, C., Bos, F., Belis, J., Lebet, J.-P. (eds.) Challenging Glass 4 EPFL University, Lausanne 2014
- Oikonomopoulou, F., Bristogianni, T., Veer, F., Nijse, R.: Developing the bundled glass column. In: Cruz, P.J.S. (ed.) Third International Conference on Structures and Architecture (ICSA 2016), Portugal 2016. CRC Press
- Oikonomopoulou, F., Veer, F.A., Nijse, R., Baardolf, K.: A completely transparent, adhesively bonded soda-lime glass block masonry system. Journal of Facade Design and Engineering 2(3-4), 201-222 (2015). doi:10.3233/fde-150021
- Schittich, C., Staib, G., Balkow, D., Schuler, M., Sobek, W.: Glass Construction Manual 2nd revised and expanded edition ed. Birkhauser, Munich (2007)
- SCHOTT: DURAN, Tubing, Capillary and Rod of Borosilicate Glass 3.3. In: AG, S. (ed.) Germany, (2012)
- SCHOTT AG: CONTURAX Product overview. In: SCHOTT (ed.), SCHOTT AG, Germany, (2013)

## Authors

F. Oikonomopoulou<sup>1\*</sup>, E.A.M. van den Broek<sup>1</sup>, T. Bristogianni<sup>2</sup>, F. A. Veer<sup>1</sup>, R. Nijse<sup>1,2</sup>

<sup>1</sup> Department of Architectural Engineering + Technology, Faculty of Architecture and the Built Environment, Delft University of Technology, Delft 2628 BL, the Netherlands

<sup>2</sup> Department of Structural Engineering, Faculty of Civil Engineering and Geosciences, Delft University of Technology, Delft 2628 CN, The Netherlands

\* contact: [f.oikonomopoulou@tudelft.nl](mailto:f.oikonomopoulou@tudelft.nl)  
[www.glass.bk.tudelft.nl](http://www.glass.bk.tudelft.nl)